Available online at www.sciencedirect.com

ScienceDirect

Current Opinion in
Colloid & Interface Science

Understanding the synthesis and reactivity of ADORable zeolites using NMR spectroscopy

Sharon E. Ashbrook, Russell Morris and Cameron M. Rice

Abstract

Zeolites remain one of the most important classes of industrial catalysts used today, and with the urgent drive for the transition from petrochemical to renewable feedstocks, there is a renewed interest in developing new types of zeolite. Recent synthetic advances in the field have included the development of the assembly-disassembly-organisation-reassembly (ADOR) method. In this short review, we will discuss how solid-state NMR experiments can be used to probe the mechanism of the process by characterising the structure of the intermediates and products, show how ^{17}O NMR spectroscopy can be used to probe the reactivity of ADORable zeolites and explain how this, in turn, can lead to fundamental questions of how zeolites behave in the presence of liquid water.

Addresses

School of Chemistry, EaStCHEM and Centre of Magnetic Resonance, University of St Andrews, North Haugh, St Andrews KY16 9ST, UK

Corresponding authors: Ashbrook, Sharon E. (sema@st-andrews.ac.uk); Morris, Russell (rem1@st-andrews.ac.uk)

Current Opinion in Colloid & Interface Science 2022, **61**:101634

This review comes from a themed issue on **NMR** 2022

Edited by **Bradley F. Chmelka** and **Anne Lesage**

For a complete overview see the Issue and the Editorial

https://doi.org/10.1016/j.cocis.2022.101634

Keywords

Solid-state NMR spectroscopy, Zeolites, ADOR, ^{17}O NMR.

Introduction

Zeolites are extremely important industrial chemicals, making up probably the most common family of heterogenous catalysis used in chemical processes today [1]. The utility of zeolites is a function of both their chemistry, which is based on fully connected tetrahedral units TO_4 of different compositions (T = Si, Al, P and a range of other elements), and their porous architectures that allow small and medium-size molecules to access the internal surface, resulting in a range of interesting chemistry. Zeolites have been particularly successful as catalysts in the oil refining and petrochemical sectors, primarily for hydrocarbon interconversions [2]. However, the transition from fossil fuel feedstocks towards renewables (such as biomass) poses different challenges [3]. Biomass-derived substrates tend to be more highly oxygenated than hydrocarbons, and this gives new challenges for optimising catalytic processes based on zeolites, including reactivity and stability issues, especially in the presence of water, which is more common in bio-based systems [4,5]. Similarly, many bio-derived substrates may be more complex polymers, and so larger porosity (or more extensive hierarchical porosity) may be required. This means there remains a great incentive to develop new zeolites based on either a different chemistry or structural topology.

The traditional method of preparing zeolites uses hydrothermal crystallisation [6]. However, in recent years, a new method for zeolite synthesis has been developed, based not on direct crystallisation but on the manipulation of a parent zeolite material through controlled partial disassembly followed by reassembly into a new structure. This mechanism is called the assembly-disassembly-organisation-reassembly (ADOR) process [7–10] and is shown schematically in Figure 1. A note on nomenclature: zeolite topologies (such as UTL, PCR and OKO as in Figure 1) are given codes by the International Zeolite Association (see iza-online.org, for further details). Individual materials are named by convention with a code plus a number indicating (usually) the name of the laboratory where the sample was made. For example, in Figure 1, IPC-*n* = Institute of Physical Chemistry.

The ADOR mechanism relies on the availability of a suitable parent zeolite, which itself is usually made by crystallisation (the assembly step). For successful application of the ADOR process, the parent zeolite should have a chemical composition that enables selective reactions to occur that disassemble this into stable building units that are terminated by silanol groups [11]. These units are then organised with respect to each other and reconnected (or reassembled) through a condensation reaction that forms SiOSi links between the units, producing a new daughter zeolite material that has a different structure to the parent. By changing the organisation step, it has been shown that several different daughter products can be prepared from the same parent, some of which would be viewed as 'unfeasible' targets using hydrothermal crystallisation [12].

Figure 1

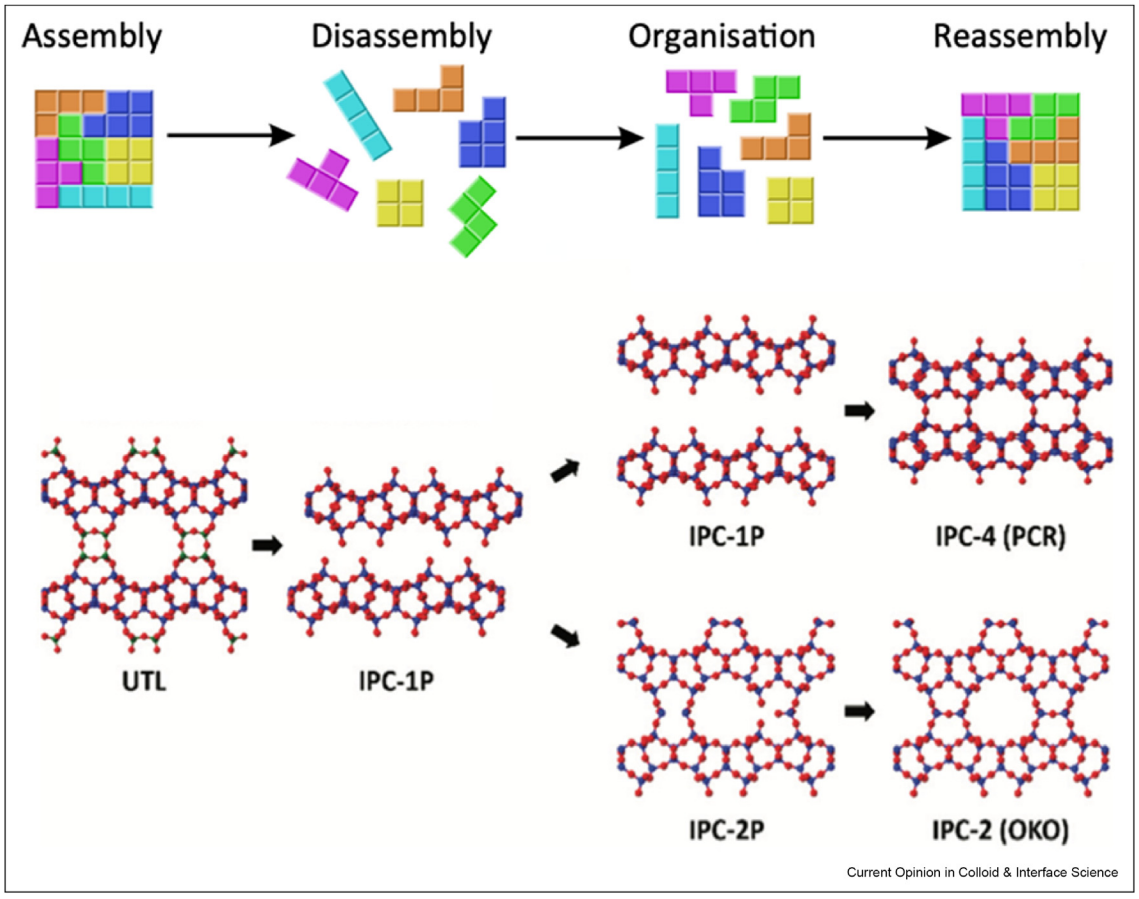

The top panel shows a schematic diagram of the design of the ADOR process. The bottom panel shows how this can be applied for the synthesis of new zeolites. A parent zeolite (in this case UTL) is assembled (A) and then hydrolytically disassembled (D) to remove the Ge-rich d4r units that link the Si-rich layers together – the material formed from this process is called IPC-1P. The resultant IPC-1P layers can then be organised (O) in such a way so as to form two new daughter zeolites, such as IPC-4 and IPC-2, by two different processes: either arranging the layers themselves to form ICP-1P or by intercalating further silicon into the interlayer region to form IPC-2P. The final zeolites are formed in the reassembly (R) step by calcination at a high temperature. Different organisation steps can lead to different final products, such as IPC-6, IPC-9 and IPC-10 (not shown).

In practice, the ADOR process is most successful when the parent zeolite is a germanosilicate with a structure that contains double four-ring (d4r) units. These units contain eight T atoms in a cubic structure and are rare in pure silica zeolites because of their slightly strained nature. However, germanium, as it is slightly larger than silicon, releases some of the strain and therefore preferentially sits in the d4r units. Figure 1 shows the zeolite UTL (zeolite topologies are named with three-letter codes, see the International Zeolite Association website, iza-online.org, for further details). UTL is a typical ADOR parent zeolite, with silica-rich layers connected through germanium-rich d4r units. The preferential location of the germanium is key as it allows one to take advantage of the difference in chemistry between silicon and germanium and, in particular, the more susceptible nature of germanium to hydrolysis. The treatment of a parent zeolite, such as UTL, with water or aqueous acid, leads to selective removal of the d4r units to leave a layered intermediate. In the case of UTL, this layered compound is given the code IPC-1P. The important point to note about this material is that the silanol groups, condensation of which will lead to the formation of the reassembled, 3D material, are formed from a fully connected parent, and are therefore perfectly arranged to return to a fully connected zeolite — but since the d4rs have been removed the structure will necessarily be different from the starting zeolite. All that has to be done is to ensure that the layers are appropriately organised relative to each other before instigating the condensation process by heating the material rapidly up to a temperature (typically around 550 °C) that drives off the water and leaves a fully connected zeolite. Figure 1 shows two ways in which this can be performed to form two new zeolites, such as IPC-4 and

IPC-2. Which of these happens in the experiment can be controlled by the use of intercalation chemistry.

However, while the ADOR process looks fairly simple at first sight, especially in the schematic form as shown in Figure 1, in real situations, it is a complex process. Zeolites are relatively dynamic materials when in contact with water (even at room temperature [13]), and during the ADOR reaction, there is the possibility for a self-organisation process to occur, where silicon is reintercalated between the layers of IPC-1P to form a new intermediate pseudo-layered material, IPC-2P (this is pseudo-layered because the intercalation of silicon leads to some of the layers being connected), and reassembly of this type of material can lead to a new set of zeolites, such as IPC-2, IPC-6 and IPC-10, depending on the exact nature of the organisation step [7,12,14]. This means the ADOR process can produce a number of daughter zeolites from the same parent, each of which has a different topology (in the case where UTL is the parent five new materials can be prepared). Since the extended layers from the parent material remain intact throughout the process [15], the phase purity of the zeolite (usually measured using powder X-ray diffraction (XRD)) is not usually a problem. However, the mechanism means that there is the possibility of significant disorder in the interlayer space, and, as is common with the stacking/reconnection of any layered material, there is the possibility of introducing stacking faults. The extent of disorder and faulting varies between materials, with some solids (such as the so-called unfeasible zeolites) being heavily faulted [12,14] while others, such as the OKO and PCR zeolites, as shown in Figure 1 [7] being quite well ordered and showing few faults.

Since the initial development of the process, several different parent zeolites with appropriate chemistry and topology have been used successfully to produce ADOR daughters [16–19]. In addition, other mechanisms of manipulation involving, for example, mechanochemistry [20] or vapour phase [21] (rather than liquid phase) hydrolysis have shown the range and importance of the ADOR process in zeolite chemistry.

Given that the ADOR mechanism is so varied and complex, an important question is how to best characterise the starting, intermediate, and final products of the process. As the initial parent and final daughter products are usually relatively crystalline, XRD is an obvious technique to use. However, during the process itself, the long-range order (e.g., the register between layers in IPC-1P) is partially, but not completely, lost and XRD, while still useful in measuring, for example, interlayer distances [22], does not give as much information as for highly crystalline solids. Other techniques, such as X-ray pair distribution function (PDF) analysis [23], positron annihilation spectroscopy [24] and computation [25] provide complementary and extremely useful information.

NMR spectroscopy is ideal for studying local structure, disorder and chemical reactivity in the solid state because of its sensitivity to the atomic-scale environment (without the need for any long-range order) [26–28]. This is particularly so for microporous materials where it provides information on both the framework and on any guest molecules incorporated in the pores or attached to metal centres [29–33]. Conventionally, rapid magic-angle spinning (MAS) is used to remove the anisotropic broadening found in NMR spectra of solids, but for nuclei with spin quantum number $I > 1/2$ (such as ^{17}O and ^{27}Al), more complex experiments (e.g., MQMAS [34,35] and STMAS [36,37]) are required to remove the quadrupolar broadening and resolve distinct species. Surface structure and chemistry can be selectively probed using magnetisation transfer approaches, such as cross-polarisation (CP) [38,39], while similar methods can also be exploited in multidimensional correlation experiments to probe through-bond connectivity and spatial proximity of nuclei, building up a detailed picture of the atomic-scale structure of the material [26–28]. Although it can be difficult to understand the complex and overlapped lineshapes that are seen in NMR spectra of disordered solids, recent advances in the first-principles computation of NMR parameters using plane-wave pseudopotential codes, such as CASTEP [40,41], have led to a step change in the quality and quantity of information available and combined NMR crystallographic approaches to understand disordered or partially disordered solids have shown their worth [42–45].

In this short paper, we will review how NMR spectroscopy can be used to characterise the parent zeolites, the intermediates and the daughter zeolites in the ADOR process and demonstrate how *in situ* NMR experiments can provide further information that helps us to understand the ADOR mechanism and the chemical reactivity of zeolites more generally.

NMR spectroscopy of parent and daughter zeolites

The key to understanding the ADOR mechanism is the detailed characterisation of its intermediates and products, and NMR spectroscopy is well suited to this task because of its sensitivity to the local structural environment. The materials appropriate for, and produced by, the ADOR process are compositionally related to SiO_2 (or hydrated SiO_2) and often contain dopant elements, such as Ge, Al, B or F. As shown in Table 1, this provides a range of opportunities to explore spatial proximity, local structure, the level and distribution of defects and chemical reactivity using NMR spectroscopy. The different nuclear spins and natural abundance of the nuclides result in sensitivity and/or resolution challenges [46], but the different position of these atoms within the structure, and their varied roles in the

Table 1

NMR properties of nuclei present in materials relevant to the ADOR process.

Nucleus	I	Natural abundance (%)	Larmor frequency at 14.1 T/MHz	Role in ADOR materials	Applicability
^{1}H	1/2	99.99	600.1	Present in water, silanols and Brønsted acid sites	Used for magnetisation transfer in CP (e.g., to Si, Al or O) and provides information on silanol formation
^{2}H	1	0.01	92.1	Present in water, silanols and Brønsted acid sites	Can reveal level of exchangeable OH and used to explore dynamics
^{11}B	3/2	80.1	192.5	Present in zeolite framework of B-substituted ADOR parents	Used to determine the preferential location of B and coordination environment
^{13}C	1/2	1.07	150.9	Present in organic SDA/ intercalates	Provides information on SDA/intercalate incorporation and form within parent or daughter zeolites
^{17}O	5/2	0.037	81.4	Present in all ADOR parents and daughters and in water used in hydrolysis	Requires (costly) isotopic enrichment but can be performed *in situ* and provides mechanistic insight through level and position of incorporation
^{19}F	1/2	100	564.7	Can be incorporated into Ge-containing zeolites	Can provide information on preferential Ge location Requires post-synthetic fluorination
^{27}Al	5/2	100	156.4	Present in zeolite framework of Al-substituted ADOR parents or daughters	Provides information on the location and distribution of Al and its coordination number
^{29}Si	1/2	4.7	119.2	Present in all ADOR parents and daughters	Characterisation of parent, intermediate and daughter zeolites and extent of disassembly/ reassembly Can require isotopic enrichment for multidimensional experiments
^{73}Ge	9/2	7.7	20.9	Present in many ADOR parent zeolites	Could indicate Ge location and distribution but a large quadrupole usually prevents easy study

reaction pathway, often determines which are the most appropriate nuclei to study and the most appropriate experiments to perform to answer a particular question of interest. The many bond breaking and forming steps in ADOR mean that the investigation of the nuclei that occupy the tetrahedrally coordinated T sites (e.g., Si, Al, B and Ge) often provide the most useful information; ^{29}Si NMR studies are the most commonly encountered.

The original and most widely studied ADORable parent zeolite is the germanosilicate UTL framework. The structure of this "extra-large pore" material is best described as a series of two-dimensional silicate sheets, connected via germanium-rich d4r units, that form 12-ring (12r) and 14-ring (14r) channels that run perpendicular to each other [47,48]. UTL is an ideal model system to study the ADOR process as it can be prepared with varying Ge content, and it is, therefore, possible to control the degree of disassembly [7,9,12,48–52]. The increased susceptibility of the Ge-O bond to hydrolysis (compared to the Si-O bond) is the origin of the controlled ADOR disassembly. As germanium is concentrated primarily in the d4r, disassembly products can be achieved reliably [53–57]. Furthermore, the two-dimensional layered silicate structure of UTL means that disassembly and reorganisation are restricted to a single dimension along the d4r-containing axis of the material, in principle allowing the mechanistic processes to be followed more easily than in germanosilicate frameworks which contain d4r in two dimensions [7,51,52,58].

The ADOR process for Ge-UTL in water or acid is reasonably well understood, with zeolite precursors, intermediates and products characterised using diffraction- and scattering-based techniques, allowing the long-range structural order to be revealed. Initial hydrolysis in hot aqueous conditions has been shown to break down the d4r units to form IPC-2P*, a short-lived and disordered germanium-containing layered material. This is rapidly converted through continued hydrolysis to IPC-1P, a disordered layered structure almost free from germanium, and where the d4r units have been removed [23,58–60]. This material may, depending on the conditions used, reintercalate aqueous silicon species from solution to form IPC-2P, a material with single four-ring (s4r) units between the zeolitic layers; however, this often requires an induction period (i.e., a time where no change is seen in the long-range order of the zeolitic layers) before such reorganisation occurs [14,22]. The intermediates in this process can be isolated and used further as they are, or other species can be intercalated. Depending on the exact treatment, a range of high-silica zeolites with novel topologies may be formed [12].

While the information on the long-range order from diffraction (e.g., the spacing of the zeolitic layers) can provide important mechanistic insight, it is not able to probe the changes to the local structure. An understanding of the interplay between the local structure and organisation/reassembly is, therefore, key to understanding the mechanistic pathways adopted under different conditions. The primary approach used to investigate this has been ^{29}Si NMR spectroscopy. As shown in Table 1, ^{29}Si has I = 1/2, and MAS and CP MAS experiments are easily implemented (despite its relatively low natural abundance). UTL has 12 crystallographically distinct T sites, giving rise to an overlapped ^{29}Si MAS NMR spectrum (see Figure 2(a)). By comparing the ^{29}Si MAS NMR spectra of a pure silica UTL with that of a germanium-substituted material, Wu and co-workers [61] were able to identify the specific region of the spectrum that corresponds to Si in d4r, as shown by the highlighted box in Figure 2(a), enabling insight into the distribution of germanium in the material and the ability to follow the degermanation process and any reintercalation of Si in the interlayer space.

The hydrolysis of UTL to form layered structures results in significant local disorder and the formation of SiOH groups at the surface of the interlayer space. ^{29}Si MAS NMR spectra of the layered IPC-xP structures should contain signals from Q^n Si species, where (4 − n) is the number of hydroxyl groups attached to the Si, which are introduced through the hydrolytic cleavage of a Si-O-Ge linkage. Recently, the ADOR process for Ge-UTL treated with hot water and acid has been followed using a combination of powder XRD and solid-state NMR spectroscopy [10,22,59]. A high-throughput sampling of the hydrolysis reaction was carried out (with samples taken every minute for the first 5 min, every 5 min for the first hour and every 30 min up to 8 h) [10]. Figure 2(a) shows ^{29}Si MAS NMR of selected samples for an ADOR reaction, and Figure 2(b) plots the variation of the d_{200} reflection position from XRD with time. As shown in Figure 2(a), the initial hydrolysis of Ge-UTL yields a material with significant Q^3 Si, indicating a very rapid and significant structural rearrangement, accompanied by a significant reduction in d_{200} spacing (Figure 2(b)) [10]. The ^{29}Si spectrum after an hour of hydrolysis exhibits a Q^3:Q^4 ratio of 1:2.3, in good agreement with the ideal ratio expected for IPC-1P (1:2.5) [62], consistent with the d_{200} spacing seen in the XRD of IPC-1P. However, upon additional hydrolysis, the material formed exhibits a Q^3:Q^4 ratio of 1:4.8, which is

Figure 2

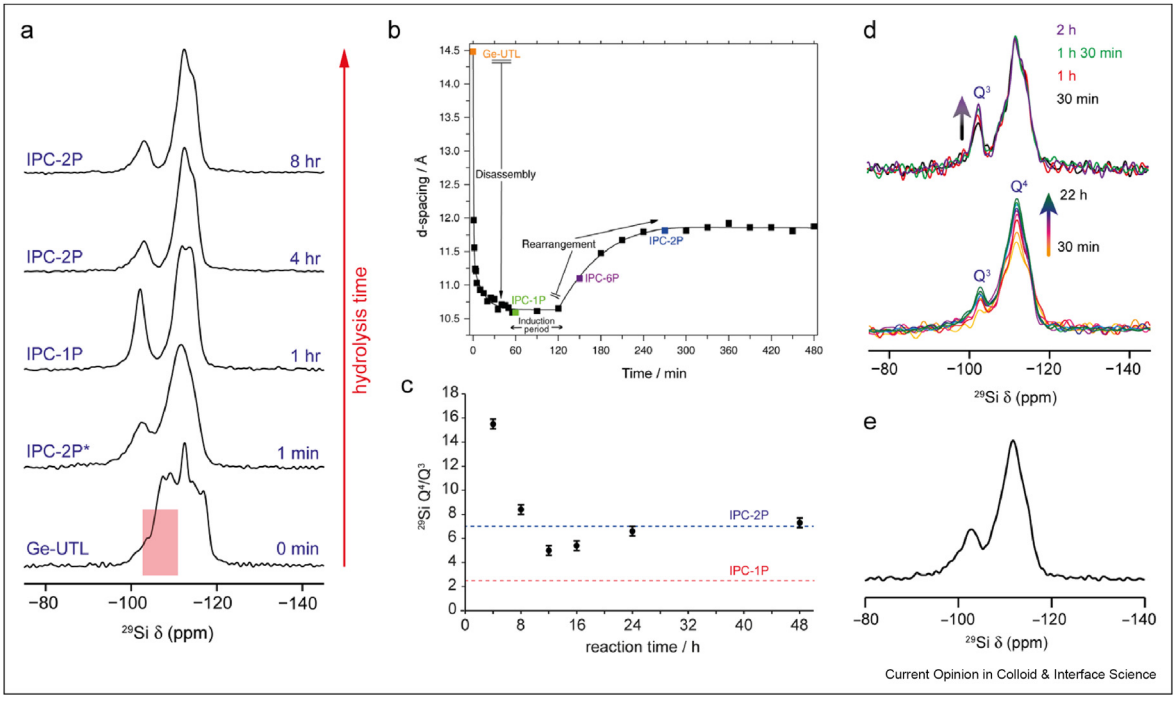

(**a**) ^{29}Si (9.4 T, 10 kHz MAS) NMR spectra and (**b**) plot of the variation in the position of the d_{200} reflection during the ADOR process for Ge-UTL hydrolysed in water at 100 °C. Reproduced from Ref. [10], with permission. (**c**) Plot of the Q^4/Q^3 intensity ratio in ^{29}Si (9.4 T, 10 kHz MAS) NMR spectra of Ge-UTL zeolite as a function of hydrolysis time at 95 °C in 6 M HCl under low-volume conditions. Adapted from Ref. [62], with permission. (**d**) ^{29}Si (9.4 T, 10 kHz MAS) NMR spectra for an ADOR hydrolysis of 18% ^{29}Si-enriched Ge-UTL carried out *in situ* at room temperature using H_2O (top) or 6 M HCl (bottom). Adapted from Ref. [63], with permission. (**e**) ^{29}Si (9.4 T, 14 kHz MAS) NMR spectrum of calcined Ge-UTL ball milled in H_2O for 30 min. Adapted from Ref. [20], with permission.

different to the value expected for ideal IPC-2P (1:7) [62] confirming that although the product at this point has the d_{200} spacing expected from the s4r between the layers, the material is much more defective on the local level. This suggests incomplete formation/connection of the s4r units.

Further investigation [22] has shown that the duration of the induction period depends on temperature, with the onset of rearrangement to IPC-2P extending (from 120 min at 100 °C) to 600 min at 81 °C and 1200 min at 70 °C. Presumably, local structural changes are taking place during this time that eventually facilitate the formation of IPC-2P. However, ^{29}Si NMR spectra of IPC-1P intermediates during the induction period show surprisingly little change in the Q^3:Q^4 ratio, suggesting it is a rearrangement of the positions of the hydroxyl groups on the surface of the zeolitic layers that is taking place, rather than a significant change in their number, perhaps ensuring the optimum alignment of these for forming the interlayer SiOSi bonds in IPC-2P.

Given the sensitivity of NMR spectroscopy to small changes in local structure, a highly desirable, but somewhat challenging, aim would be to follow the ADOR reaction *in situ* (i.e., inside the NMR rotor), enabling the local structure to be monitored directly under the reaction conditions. This, however, places very strict limits on the volume of the reaction that can be used (the NMR rotor has an external diameter of 4 mm if MAS rates of 10−14 kHz are desired), and this is further compromised by the requirement to combine the solid and hydrolysing solution inside a sealed PTFE HRMAS insert, placed inside the rotor, to ensure stable spinning. Plots of the ^{29}Si Q^4/Q^3 ratio from Ge-UTL materials hydrolysed *ex situ* in low-volume conditions (2.4 mL of 6 M HCl) at 95 °C showed that this change in volume (both in absolute terms and the reduction in the relative amount of acid) resulted in significant changes, with a much slower rate of initial hydrolysis [62]. As shown in Figure 2(c), a plot of the Q^4/Q^3 intensity ratio against time, the initial hydrolysis now occurs over 8−12 h, and IPC-1P is never really fully formed before the rearrangement to IPC-2P begins to dominate.

The low volume required for an *in situ* reaction results in poor spectral sensitivity, particularly for ^{29}Si, which has a natural abundance of 4.7%, and the extensive signal averaging that would usually be employed may not be feasible on the timescale of the ADOR reaction. This can be overcome (at some cost) by preparing the UTL using isotopically enriched ^{29}Si, which then enables the reaction to be followed in real time. Figure 2(d) shows ^{29}Si MAS spectra acquired *in situ* during ADOR reactions carried out at room temperature and reacting 20 mg of 18% ^{29}Si-enriched UTL with 10 μL of either distilled water or 6 M HCl [63]. When water is used an increase in the Q^3 signal is seen relatively quickly (over the first 2 h of reaction), indicating the removal of Ge and loss of the d4r units. The reaction is more rapid when acid is used, and the organisation process (and subsequent growth of Q^4 Si species as IPC-2P is formed) can then be followed over 24 h as shown in Figure 2(d). The increase in Q^4 Si arises from the reintercalation of Si (originally located in the d4r) from solution, and the layers become reconnected. ^{29}Si NMR (of samples hydrolysed *ex situ*) [63] revealed that the local structure continued to change even after the final interlayer spacing of IPC-2P has been reached, with the Q^4/Q^3 ratio increasing from ∼4 at 24 h (when XRD suggests IPC-2P is fully formed) to the expected ∼7 only after 48 h, cautioning against the use of only a single technique to probe the reaction and the products formed.

A key target in ADOR experiments is the development of sustainable and scalable methods for the disassembly and organisation steps, with a view to increasing the economic and industrial viability of the process. A significant reduction in the solvent and the reaction time is desirable, and several approaches, employing mechanochemical synthesis, high-pressure reactions, hydrogen-reduction and vapour-phase syntheses, have been explored [20,22,64,65]. Ge-UTL was successfully hydrolysed at room temperature with significantly reduced solvent, and at very short reaction times (maximum 30 min) using mechanochemistry (150 rpm) [20]. ICP-2, IPC-6 and IPC-4 materials were obtained depending on the acid concentration, and notably without complete disassembly to IPC-1P. However, the materials exhibit a greater degree of disorder compared to those from conventional syntheses, as shown in the ^{29}Si MAS NMR spectrum of a mechanochemically prepared IPC-2P in Figure 2(e). This spectrum exhibits broader lines than expected, and a Q^4/Q^3 ratio of 3.1, closer to that expected for IPC-1P rather than the IPC-2P (despite the material exhibiting the d-spacing for the latter). High-pressure, high-temperature (1 GPa, 200 °C) treatment of IPC-1P resulted in the unexpected formation of IPC-2, a less-dense material than the IPC-4 obtained by conventional calcination [64]. The formation of siliceous s4r in the interlayer space in the absence of additional silicon implies that silicon from the zeolitic layers relocates to populate this region. ^{29}Si CP MAS and MAS NMR spectra show evidence of Q^3 species, confirming the presence of a defective IPC-2 phase (with a total silanol content of 10%). The degermanation of UTL using controlled hydrogen reduction produced a range of siliceous ADOR daughter zeolites, depending on the initial reduction conditions [65]. ^{29}Si NMR spectra revealed that the length of the hydrogen reduction treatment affected the degermanation level (and the Si/Ge ratio) and the presence of Q^3 and Q^2 Si, owing to the fact that silicon migration, as seen in solution, is not likely.

ADOR reactions on zeolites other than UTL have also been carried out. Recently, Kasneryk et al. produced

Figure 3

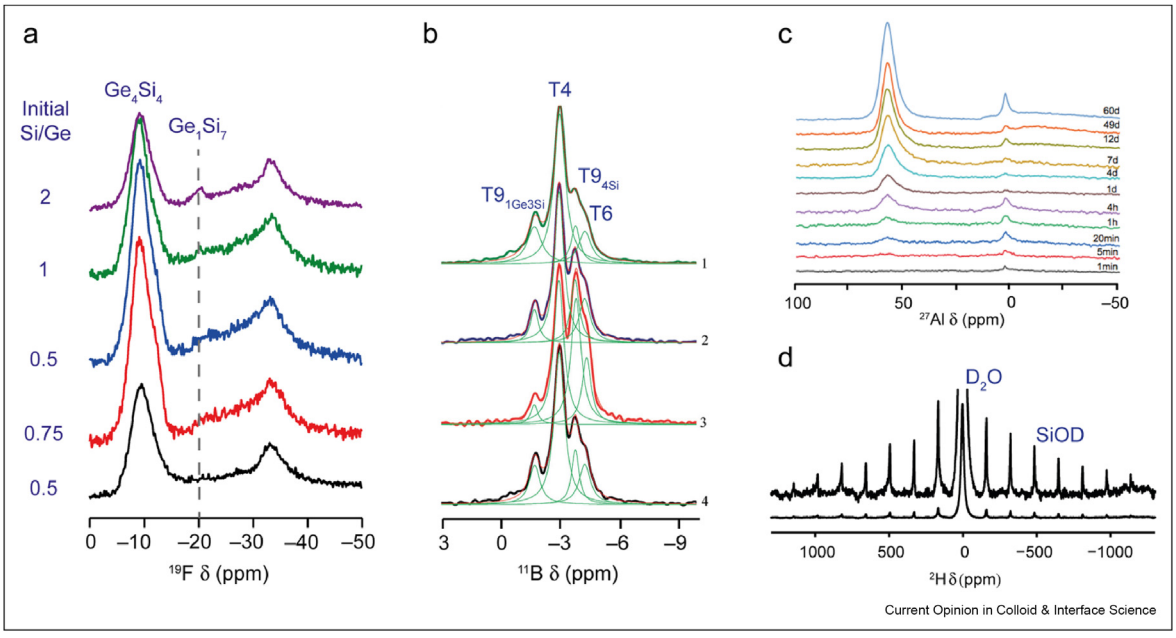

(**a**) ^{19}F (14.1 T, 25 kHz MAS) NMR spectra of calcined post-synthetically fluorinated Ge-UOV synthesised with varying Si/Ge ratio. Adapted from Ref. [17]. (**b**) ^{11}B (11.7 T) MAS NMR spectra hydrothermally prepared Ge,B-UTL, with varying concentrations of boron included in the synthesis. Reprinted (adapted) with permission from Ref. [71]. Copyright 2011 American Chemical Society. (**c**) ^{27}Al (9.4 T, 15 kHz MAS) NMR spectra of Al-UTL prepared during ADOR transformation of Ge-UTL and heated for varying times. Reprinted (adapted) with permission from Ref. [74]. Copyright 2021 American Chemical Society. (**d**) ^{2}H (9.4 T, 10 kHz MAS) NMR spectrum of a deuterated hydrolysed (16 h) Ge-UTL zeolite, with an expansion to show the broad spinning sideband manifold. Reprinted (adapted) with permission from Ref. [62]. Copyright 2017 American Chemical Society.

new daughter zeolites through an ADOR transformation of germanosilicate IWW, using vapor-phase transport [21], with ^{29}Si NMR used to follow the formation of the novel IPC-18P precursor and the novel zeolitic calcined product IPC-18. ^{29}Si NMR has also been used in the analysis of ADOR materials derived from UOV and *CTH parent zeolites [19,52,66]. For example, the ADORable zeolite SAZ-1 (*CTH), containing germanium-rich d4r units, was disassembled to a layered precursor SAZ-1P which can be annealed to give two novel zeolites, such as IPC-15 and IPC-16, depending on the calcination conditions [19]. The comparison of ^{29}Si MAS NMR spectra to those of IPC-1P and IPC-2P reveals a comparably high level of silanols present in SAZ-1P. Calcination produces the two novel zeolites with comparable defect levels to those seen in UTL-derived IPC-2 and IPC-4.

A key prerequisite for a successful ADORable zeolite is a high concentration of germanium in strained framework units (such as d4r), located between porous, highly siliceous two-dimensional layers, allowing selective disassembly and organisation. It is useful, therefore, to assess the location and distribution of germanium with a zeolitic framework. In conjunction with conventional XRD measurements (which can provide the average composition of an atomic site), this is often studied using ^{19}F NMR spectroscopy, with post-synthetic fluorination resulting in the occlusion of fluorine within d4r units. The ^{19}F chemical shift is then sensitive to the number of next-nearest neighbour (NNN) silicon or germanium atoms within the d4r [67–69]. The use of ^{19}F NMR (I = 1/2, 100%) is significantly easier than probing the Ge distribution directly using ^{73}Ge NMR spectroscopy, owing to the very large quadrupolar broadening this typically exhibits (see Table 1). Figure 3(a) shows ^{19}F MAS NMR spectra of a parent UOV zeolite, prepared using different Si/Ge ratios in the starting gel [17]. Although the final UOV-derived products had very similar Si/Ge ratios (3.1–3.3) irrespective of the initial composition, ^{19}F NMR spectroscopy revealed some subtle differences in the Ge distribution. ^{19}F spectra of all materials showed two major signals; one at −10 ppm (assigned to F^- occluded in Ge_4Si_4 rings) and one at −30 ppm, typically assigned to F^- in the siliceous layer. However, a gradual increase in the intensity of a signal at −20 ppm, attributed to F in Ge_1Si_7 rings, was observed with increasing Si/Ge ratio. This was shown to prevent the successful formation of the daughter zeolite IPC-12, leading to low lability interlayer regions. Similarly, the presence of hydrolytically stable Ge_1Si_7 units in an ITH parent zeolite (even at reasonably high levels of Ge incorporation) was shown to significantly hinder the lability of the structure [70].

The inclusion of germanium in a parent zeolite provides the possibility of producing frameworks with topologies that contain constrained units (e.g., d4r) or extra-large pores (e.g., 12r or 14r). Owing to the high cost of germanium precursors, such as GeO_2 or $Ge(OEt)_4$, there is also a drive to replace some or all of the Ge with other framework atoms, such as B or Al. These trivalent atoms produce a negatively charged framework, resulting in the possibility of additional Brønsted acid sites. The inclusion of B in UTL has been achieved under a range of conditions [69,71,72]. ^{11}B NMR spectroscopy has been able to reveal the preferential locations of B within the framework, as shown in Figure 3(b), which shows ^{11}B MAS NMR spectra of B,Ge-UTL prepared with different initial concentrations of B [71]. The final concentration of B in the zeolite did not change significantly with any increase in the starting reagents; however, increasing the B content did result in a higher Si/Ge ratio (i.e., less Ge being incorporated). The authors demonstrated that the ^{11}B spectra could be decomposed into four components and that the intensities of these varied with Si/Ge ratio. By comparison to DFT calculations to determine the most energetically favourable positions for B substitution, it was determined that when there are low levels of B in the starting gel, this is incorporated into the final zeolite at the T4 and T9 positions and in lower levels into T6. As the Ge content of the final product decreases, additional B is seen in the T9 position. Similar work using ^{27}Al NMR has investigated the loading and distribution of Al in germanosilicate zeolites, providing information on the preferences for Al siting, and the level of Al retained in the framework after ADOR hydrolysis. In general, Al incorporation has proven more difficult than for other framework elements, and more often, a post-synthetic incorporation approach has been employed. The successful incorporation of Al into the zeolite framework can be confirmed by the presence of signals corresponding to tetrahedrally coordinated Al (at 50–60 ppm), and this has been shown for ADOR daughter zeolites of ITH, IWW, UTL and UOV frameworks [12,49,66,72–74]. In recent work, however, post-synthetic alumination successfully produced tetrahedrally coordinated framework Al in the parent UTL structure through the reassembly of siliceous layers in the presence of Al [74]. This reaction was followed using ^{27}Al NMR, with framework Al species evident after 1 h of reaction, as shown in Figure 3(c). This use of the ADOR reaction may facilitate the design and synthesis of previously predicted, but currently inaccessible, Al-containing zeolites.

^{17}O NMR spectroscopy of zeolite frameworks

One nucleus with significant potential in solid-state NMR spectroscopy of ADOR parents, intermediates and daughters is ^{17}O. Oxygen is a key component of the zeolite framework, and ^{17}O NMR provides information on framework composition through the nature of the two directly bound atoms, Brønsted acid sites and the silanols/germanols created by hydrolysis, which line the surfaces of the layered intermediates. ^{17}O, however, has been much less commonly studied using NMR spectroscopy than, e.g., ^{29}Si, because of its quadrupolar nature (I = 5/2), which complicates the acquisition of high-resolution spectra, and it has an extremely low natural abundance of 0.037%, as shown in Table 1 [33,46]. To acquire spectra on a reasonable timescale requires isotopic enrichment, although this can be costly, and often necessitates changes to synthetic procedures (both in terms of the number/type of steps used and the scale at which a reaction is performed) [33]. However, the ability to introduce isotopically enriched reagents at different points in the ADOR pathway provides a unique insight into the mechanism of the process.

^{17}O NMR spectroscopy was first used to follow the ADOR process by Bignami et al. in 2017 [62]. Although the hydrolysis of a Ge-UTL (18% ^{29}Si enriched) was carried out *ex situ* in 6 M HCl solution for 16 h, this was performed at small volume, both to reduce the amount of costly isotopically enriched water required and with a view to future *in situ* reactions. As shown in Figure 4(a), the ^{17}O MAS spectrum of the IPC-2P product shows more than one chemically different type of O species is present, and SiOSi and SiOH signals can be resolved using MQMAS experiments (although high-power ^{1}H decoupling is required to see the latter, as shown in Figure 4(b)). Interestingly, the MAS spectrum shows small changes in the lineshape during the time the sample was studied (over 30 days), indicating a low level, ongoing hydrolysis and rearrangement process. This suggests some water is retained in the interlayer space (despite the prior drying of the sample), and this was confirmed by ^{2}H MAS NMR spectra of a deuterated hydrolysed sample. The spectrum (as shown in Figure 3(d)) reveals a sharp resonance from D_2O, and an extensive sideband manifold from SiOD groups (C_Q = 80–100 kHz). The relative intensities of the two signals suggest up to four D_2O molecules per SiOD group are present in the interlayer space, with rapid isotropic tumbling of the water molecules (and likely H exchange between water and silanols) accounting for the poor CP signal observed for SiOH in the protonated sample. The relative proportions of SiOSi, SiOH and H_2O species were obtained from a quantitative ^{17}O MAS spectrum (acquired with a short flip angle). The 8:1 SiOSi:SiOH ratio observed indicates that ^{17}O is incorporated not just into the interlayer space but, perhaps more unexpectedly, also into the bulk of the zeolitic layers and suggests a much more extensive ADOR rearrangement process than previously expected (Figure 4(c)). This was further investigated using two-dimensional ^{17}O/^{29}Si D-HMQC spectra (Figure 4(d)) of the doubly enriched hydrolysis product, which

Figure 4

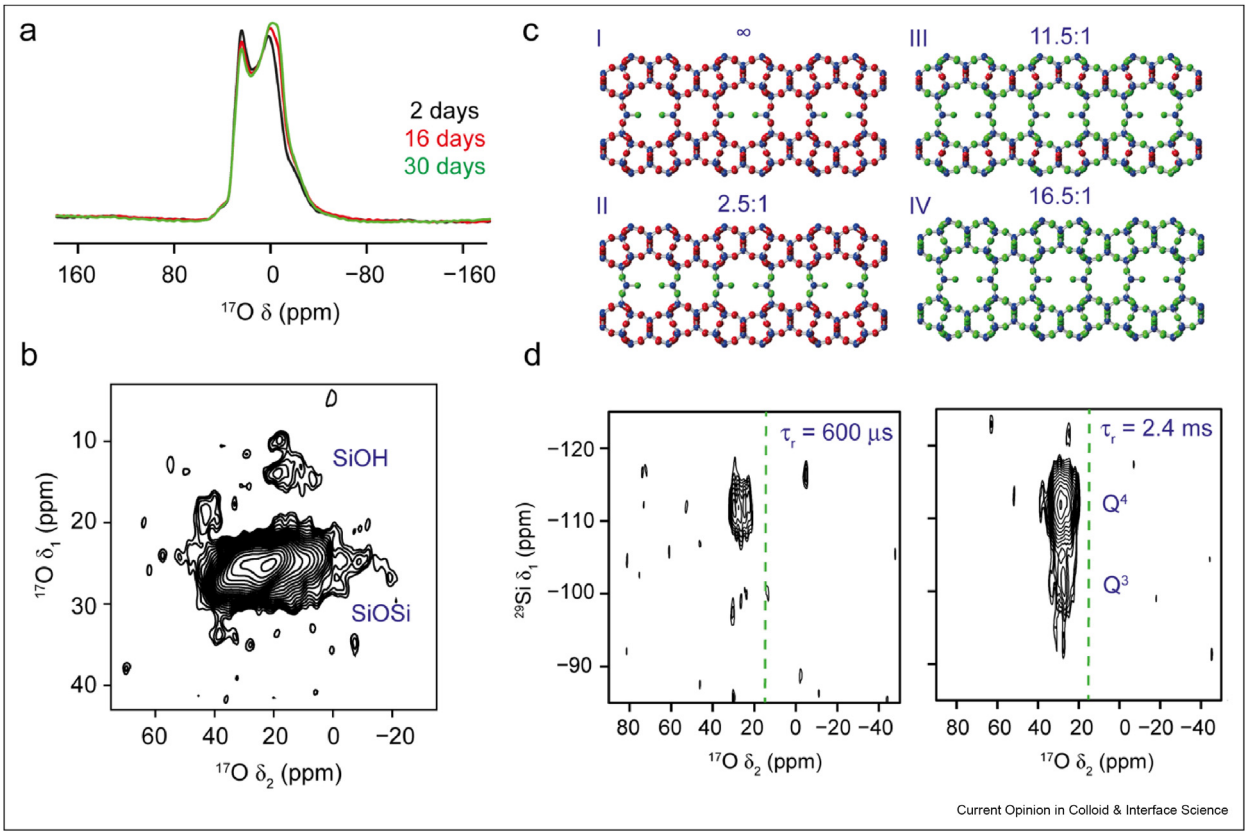

NMR spectra of ^{29}Si-enriched Ge-UTL hydrolysed with an ^{17}O-enriched solution of 6 M HCl for 16 h. (**a**) ^{17}O (14.1 T, 20 kHz MAS) NMR spectra acquired 2 (black), 16 (red) and 30 (green l) days after synthesis. (**b**) ^{17}O (20.0 T, 20 kHz MAS) MQMAS NMR spectrum acquired with high-power ^{1}H decoupling. (**c**) Schematic showing hypothetical models of possible ^{17}O incorporation (green spheres) into idealised IPC-2P, showing the expected SiOSi/SiOH ratios. (**d**) ^{17}O–^{29}Si (20.0 T, 20 kHz MAS) D-HMQC correlation spectra, acquired using τ = 600 μs and 2400 μs of SR^2_{41} recoupling. The dashed green line denotes the position of Si–OH species in the CP MAS spectrum. Reprinted (adapted) with permission from Ref. [62]. Copyright 2017 American Chemical Society.

showed a correlation between the SiOSi oxygens in the zeolitic layers and Q^4 Si at short recoupling times, but an additional correlation to the Q^3 Si in the interlayer spaced only at longer recoupling times, confirming the spatial separation of these two types of species. Note the rapid relaxation of SiOH ^{17}O signals means that these do not appear in the HMQC spectrum (but these are present in and can be quantified from the MAS spectrum).

We have carried out a range of ADOR hydrolyses with ^{17}O enriched water using a variety of different conditions, including lower/higher volumes, differing relative levels of water, different levels of acidity (and simply using water) and at a variety of temperatures, enabling, in principle, the reaction rates and nature of the intermediates/products to be followed using ^{17}O NMR [20,62]. As an example, Figure 5(a) shows the ^{17}O MQMAS spectrum of a sample of Ge-UTL ball milled in $H_2{}^{17}O$ at room temperature for 2 h [20]. Mechanochemistry provides an interesting opportunity for ^{17}O enrichment of the ADOR starting materials, intermediates or products in a cost-effective and atom-efficient way, owing to the use of very limited amounts of enriched reagents (as shown more generally for oxides, hydroxides, carboxylic acids, amino acids and silica surfaces in recent work [75–77]). In the example, as shown in Figure 5, 100 μL of water was used to hydrolyse 500 mg of Ge-UTL, leading to an estimated overall enrichment level of ∼10% (in good agreement with the level of ^{17}O present in all reagents and starting materials). Even with this relatively low amount of water (and no acid), the zeolite is successfully disassembled, and subsequently reassembled to an IPC-2-like material. An ^{17}O MQMAS spectrum reveals the enrichment of SiOSi and SiOGe signals (although these are significantly overlapped and can only be identified using multiple field measurements) and a significant amount

Figure 5

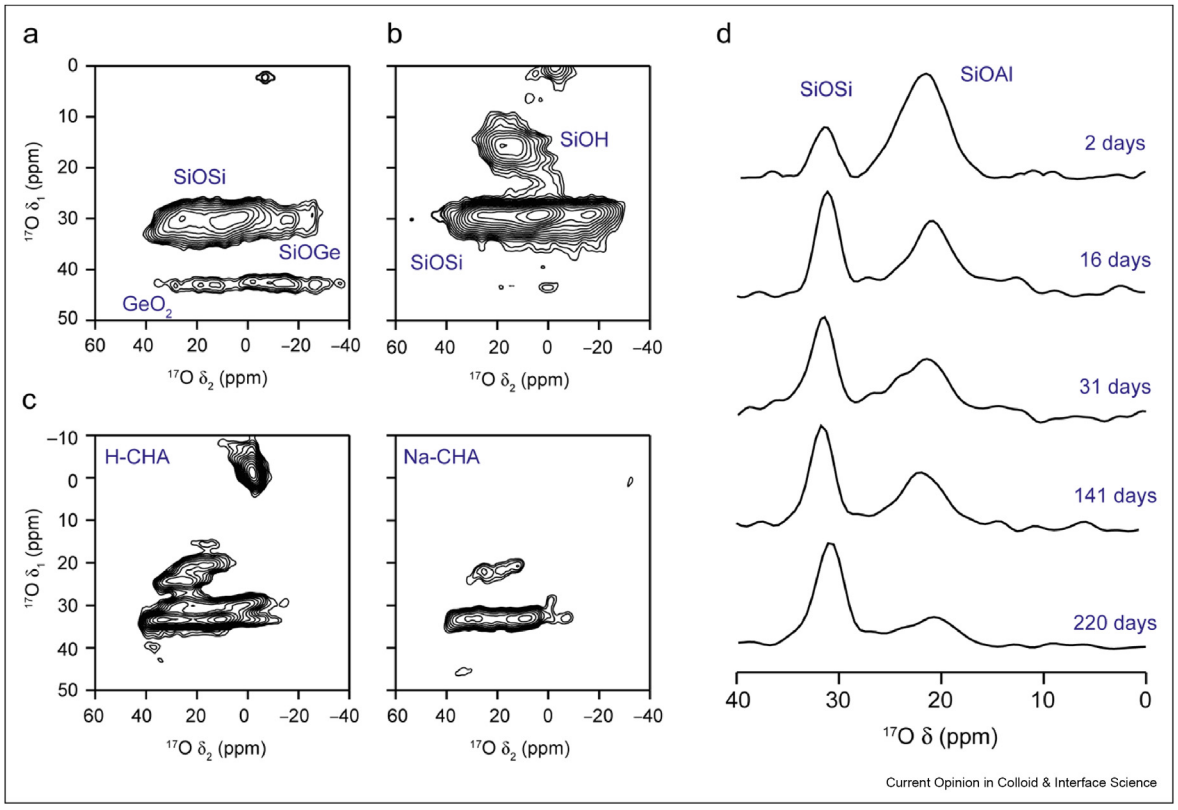

(**a**) ^{17}O (14.1 T, 14 kHz MAS) MQMAS NMR spectrum of Ge-UTL ball-milled in 100 μL of $H_2^{17}O$(l) at room temperature for 2 h [20]. (**b**) ^{17}O (14.1 T, 14 kHz MAS) MQMAS NMR spectrum of Ge-UTL heated in 6 M HCl at 92 °C for 24 h, dried and then exposed to 100 μL of $H_2^{17}O$(l). (**c**) ^{17}O (14.1 T, 14 kHz MAS) MQMAS NMR spectra of SSZ-13 H-CHA and Na-CHA slurried *in situ* with $H_2^{17}O$(l) for 47 and 115 days, respectively [13]. (**d**) Projections of ^{17}O MQMAS NMR spectra of H-MOR slurried *in situ* with $H_2^{17}O$(l) for varying time. Reprinted (adapted) with permission from Ref. [80]. Copyright 2020 American Chemical Society.

of GeO_2 [20,78]. Although this latter species has been identified in previous ADOR reactions, in the more traditional synthesis when large volumes of solvent are used, this is recyclable within the reaction [79]; however, this is not the case here where the level of solvent is significantly lower. Despite this low level of solvent, a high level of ^{17}O incorporation into the silicate layers is observed. Interestingly, we have also seen ^{17}O enrichment of SiOSi in UTL with little or no germanium present (Si/Ge ≈ 120), perhaps suggesting the bond lability results, at least in part, from the zeolite framework itself, rather than purely from the presence of germanium or from the ADOR conditions. This can also be seen in Figure 5(b), an ^{17}O MQMAS spectrum of Ge-UTL hydrolysed in 6 M HCl at 92 °C for 24 h in high volumes of (unenriched) solvent, and subsequently dried, before being mixed with 100 μL of $H_2^{17}O$ (which is simply dropped onto the solid at room temperature). The ADOR conditions employed should remove all Ge from the intermediate IPC-2P phase, yet high levels of ^{17}O enrichment can be still seen, not just of the SiOH groups (as perhaps expected) but also of the SiOSi oxygens. Again, this suggests it is the zeolite framework itself that is labile, even simply upon exposure to water at room temperature.

The precise mechanism of the dynamics and lability of the zeolites in the ADOR process is still under study, but the greater than expected framework lability seen in ADOR raises the more general, but perhaps more interesting, the question of whether zeolites can indeed be thought of as inert scaffolds in contact with aqueous solutions. However, any ADOR intermediate or product could potentially still contain small amounts of germanium and/or exhibit a higher level of defects, depending on the reactions that have produced it. Therefore, the surprising zeolitic bond lability upon exposure to water has further investigated using conventional aluminosilicate zeolites [13,80]. As shown in Figure 5(c), rapid ^{17}O enrichment of the framework was seen when the acid form of a CHA zeolite (SSZ-13) was slurried at room temperature with a small volume

(25 μL) of $H_2{}^{17}O$ inside the NMR rotor [13]. Even after just a few hours, ^{17}O MQMAS spectra can be easily collected and reveal enrichment of both SiOAl and SiOSi oxygens. While the lability of the SiOAl bonds might be less unexpected, owing to their more acidic nature, significant enrichment at room temperature of the SiOSi bonds is certainly more surprising. It is clear, however, that the enrichment of SiOAl species is more rapid, with the $Si^{17}OAl/Si^{17}OSi$ intensity ratio decreasing from 0.5 after 1 day to the ideal value of ∼0.1 after ∼150 days [13]. A similar result can also be seen in Figure 5(d) for a MOR zeolite that has been treated similarly [80]. Although ^{17}O enrichment of the chemically different O species is seen even after 1 day, there is a clear preference for SiOAl enrichment at short slurrying times. However, the work in Ref. [80] for both MOR and FER confirms that rapid enrichment is seen for zeolites with different framework topologies, and that this phenomenon is not simply a function of the CHA topology. Ab initio molecular dynamics simulations (using a CHA model with $15H_2O$ molecules within a cell with 36 T sites and Si/Al of 11) showed that breaking the SiOAl bond required an interaction with just a single water molecule (giving an activation energy of 20–30 kJ mol^{-1} at 300 K) [13]. A room-temperature accessible barrier was also seen for SiOSi bond breakage (∼60 kJ mol^{-1}), but, in contrast, this required a hydrogen-bonded chain of at least three water molecules and a "Grotthuss-type" proton shuffling along the chain. This novel "axial" mechanism, with the Si-O bond breaking in an anti-position to the adsorbed water, was predicted to be possible for three of the four crystallographic oxygens (O1, O3 and O4) in CHA, perhaps explaining the slower enrichment seen experimentally for some signals in the ^{17}O spectrum [13].

Although, in ongoing work, we have seen similarly rapid ^{17}O enrichment for zeolites with different topologies and different levels/distributions of Al, the role played by the Brønsted acid H in any framework lability (and how important this is for the rate of exchange) is still unclear. In some cases, reasonably rapid enrichment can still be seen for ion-exchanged zeolites (e.g., Na-MOR in Ref. [80] and Na-CHA as in Figure 5(c)), but there is anecdotal evidence that this is often slower (although in absolute terms still surprisingly rapid given the lack of Brønsted acid protons and the low temperature). It is also notable that the enrichment of some purely siliceous zeolites (e.g., CHA) is also possible, where there is no Brønsted acidity at all. However, for other ion-exchanged zeolites, although enrichment occurs over longer times, it is clearly much slower and at a lower level. Interestingly, different rates of enrichment can be seen for ion-exchanged zeolites that are supposedly chemically similar but have been prepared/exchanged in different ways. This suggests that framework lability with water results not just from the chemical structure and topology, but perhaps also from the presence and nature of the defects present (e.g., residual acid H or SiOH groups, even though these are clearly not at any significant level), and that the chemical reactivity of a zeolite framework is likely to be dependent on how exactly it has been prepared and treated. While this recent work has perhaps raised more questions than it has answered, it seems clear that NMR spectroscopy (and ^{17}O NMR spectroscopy in particular) offers a unique opportunity to explore the lability and flexibility of zeolites (whether conventional or ADORable), and ultimately their chemical reactivity in solution-based processes, in a more systematic way in the future.

Conclusions and outlook

The ADOR process, and the range of novel materials it can produce, offers new opportunities in zeolite synthesis. As the process is not a reversible crystallisation like the majority of hydrothermal zeolite preparations, there is the potential for making new materials that are not possible using the traditional mechanisms. The synthesis of such 'unfeasible' zeolites (as they have been termed) is now a realistic possibility and further research is ongoing.

However, the complexity of the process leads to real challenges in understanding the mechanism, what controls the intermediates and daughter products that can be produced and, ultimately, how the approach can be better controlled to selectively design functional solids with specific properties. An understanding not just of the long-range order, but also of the detailed local structure, is vital for insight into how the surfaces of the zeolitic layers can be manipulated, functionalised and reconnected. NMR spectroscopy provides a unique insight into this detailed structure and should be the perfect complement to diffraction and other techniques in these systems. Its element-specific nature allows species to be studied selectively, and its sensitivity to motion enables investigation, not just of the atomic-scale structure, but also of dynamics and chemical reactivity. Recent work using ^{17}O, which can be introduced at a variety of specific points within the mechanistic pathway, provides additional and exciting possibilities for deepening and widening understanding, in addition to simply improving NMR sensitivity. The number of publications that really exploit advanced NMR techniques to understand the ADOR process, and the daughter zeolites produced is still relatively small, but as the complexity of the reactions carried out using this approach increases (e.g., with greater functionalisation of the interfaces and surfaces), NMR will become an increasingly important tool. It is also likely that more conventional NMR experiments will become further supplemented by (i) techniques with increased surface selectivity such as dynamic nuclear polarisation (DNP) [81–84] which also has additional sensitivity benefits, although *in situ* studies may be more challenging using

this approach owing to the specific conditions under which it is carried out and (ii) more advanced computational approaches, e.g., first-principles calculations and molecular dynamics [42–45]. Inspired by the mechanistic insight from studies of the ADOR process, ^{17}O NMR is also making a significant contribution to our understanding of the unexpected lability of zeolites when in contact with aqueous solutions. This work shows the value of developing routes for isotopic enrichment and the development of experiments that exploit such enrichment in these materials. The richness of the information available from such studies offers great potential for a better understanding of the practical mechanisms in which these important solids are involved as well as their fundamental properties.

Declaration of competing interest

The authors declare that they have no known competing financial interests or personal relationships that could have appeared to influence the work reported in this paper.

Acknowledgements

The authors would like to thank the ERC (EU FP7 Consolidator Grant 614290 EXONMR and Advanced Grant 787073 ADOR) and EPSRC (EP/N509759/1) for a studentship for CMR. The research data (and/or materials) supporting this publication can be accessed at https://doi.org/10.17630/d82e58e4-b4a0-40b3-8156-5cbf80ecea72 [85].

References

Papers of particular interest, published within the period of review, have been highlighted as:

* * of outstanding interest

1. Vermeirin W, Gilson J-P: **Impact of zeolites on the petroleum and petrochemical industry**. *Top Catal* 2009, **52**:1131–1161, https://doi.org/10.1007/s11244-009-9271-8.

2. Yilmaz B, Müller U: **Catalytic applications of zeolites in chemical industry**. *Top Catal* 2009, **52**:888–895, https://doi.org/10.1007/s11244-009-9226-0.

3. Kubicka D, Kikhtyanin O: **Opportunities for zeolites in biomass upgrading. Lessons from the refining and petrochemical industry**. *Catal Today* 2015, **243**:10–22, https://doi.org/10.1016/j.cattod.2014.07.043.

4. Ennaert T, van Aelst J, Dijkmans J, De Clercq R, Schuyster W, Dusselier M, Verboekend D, Sels BF: **Potential and challenges of zeolite chemistry in the catalytic conversion of biomass**. *Chem Soc Rev* 2016, **45**:584–611, https://doi.org/10.1039/C5CS00859J.

5. Jacobs PA, Dusselier M, Sels BF: **Will zeolite-based catalysis be as relevant in future biorefineries as in crude oil refineries?** *Angew Chem* 2014, **53**:8621–8626, https://doi.org/10.1002/anie.201400922.

6. Cundy CS, Cox PA: **The hydrothermal synthesis of zeolites: history and development from the earliest days to the present time**. *Chem Rev* 2003, **103**:663–702, https://doi.org/10.1021/cr020060i.

7. * * Roth WJ, Nachtigall P, Morris RE, Wheatley PS, Seymour VR, Ashbrook SE, Chlubná P, Grajciar L, Položij M, Zukal A, Shevts O, Čejka J: **A family of zeolites with controlled pore size prepared using a top-down method**. *Nat Chem* 2013, **5**:628–633, https://doi.org/10.1038/nchem.1662.
Original publication detailing the invention of the ADOR process.

8. Chlubna-Eliasova P, Tian Y, Pinar AB, Kubů M, Čejka J, Morris RE: **The assembly-disassembly-organization-reassembly mechanism for 3D-2D-3D transformation of germanosilicate IWW zeolite**. *Angew Chem Int Ed Engl* 2014, **53**:7048–7052, https://doi.org/10.1002/anie.201400600. 2014.

9. Eliasova P, Opansenko M, Wheatley PS, Shamzhy M, Mazur M, Nachtigall P, Roth WJ, Morris RE, Čejka J: **The ADOR mechanism for the synthesis of new zeolites**. *Chem Soc Rev* 2015, **44**:7177–7206.

10. Henkelis SE, Mazur M, Rice CM, Bignami GPM, Wheatley PS, Ashbrook SE, Čejka J, Morris RE: **A procedure for identifying possible products in the assembly-disassembly-organization-reassembly (ADOR) synthesis of zeolites**. *Nat Protoc* 2019, **14**:781–794, https://doi.org/10.1038/s41596-018-0114-6.

11. Morris RE, Čejka J: **Exploiting chemically selective weakness in solids as a route to new porous materials**. *Nat Chem* 2015, **7**:381–388, https://doi.org/10.1038/nchem.2222.

12. Mazur M, Wheatley PS, Navarro M, Roth WJ, Položij M, Mayoral A, Eliasova P, Nachtigall P, Čejka J, Morris RE: *Nat Chem* 2016, **8**:58–62, https://doi.org/10.1038/nchem.2374.

13. * * Heard CJ, Grajciar L, Rice CM, Pugh SM, Nachtigall P, Ashbrook SE, Morris RE: **Fast room temperature lability of aluminosilicate zeolites**. *Nat Commun* 2019, **10**:4690, https://doi.org/10.1038/s41467-019-12752-y.
Using ^{17}O NMR spectroscopy to demonstrate the surprising lability of zeolites even at room temperature in the presence of water.

14. Wheatley PS, Chlubna-Eliasova P, Greer H, Zhou W, Seymour VR, Dawson DM, Ashbrook SE, Pinar AB, McCusker LB, Opansenko M, Čejka J, Morris RE: **Zeolites with continuously tuneable porosity**. *Angew Chem Int Ed Engl* 2014, **53**:13210–13214, https://doi.org/10.1002/anie.201407676.

15. Clubna P, Roth WJ, Greer HF, Zhou W, Shevts O, Zukal A, Čejka J, Morris RE: **3D to 2D routes to ultrathin and expanded zeolitic materials**. *Chem Mater* 2013, **25**:542–547, https://doi.org/10.1021/cm303260z.

16. Kasneryk V, Shamzhy M, Opanasenko M, Wheatley PS, Morris SA, Russell SE, Mayoral A, Trachta M, Čejka J, Morris RE: **Expansion of the ADOR strategy for the synthesis of zeolites: the synthesis of IPC-12 from zeolite UOV**. *Angew Chem Int Ed Engl* 2017, **56**:4324–4327, https://doi.org/10.1002/anie.201700590.

17. Kasneryk V, Shamzhy M, Opanasenko M, Wheatley PS, Morris RE, Čejka J: **Insight into the ADOR zeolite-to-zeolite transformation: the UOV case**. *Dalton Trans* 2018, **47**:3084–3092, https://doi.org/10.1039/C7DT03751A.

18. Vesely O, Eliasova P, Morris RE, Čejka J: **ADOR: reconstruction of UTL zeolite from layered IPC-1P**. *Mater. Adv.* 2021, **2**:3862–3870, https://doi.org/10.1039/D1MA00212K.

19. Firth DS, Morris SA, Wheatley PS, Russell SE, Slawin AMZ, Dawson DM, Mayoral A, Opanasenko M, Položij M, Čejka J, Nachtigall P, Morris RE: **Assembly-Disassembly-Organization-Reassembly synthesis of zeolites based on cfi-type layers**. *Chem Mater* 2017, **29**:5605–5611, https://doi.org/10.1021/acs.chemmater.7b01181.

20. * * Rainer DN, Rice CM, Warrender SJ, Ashbrook SE, Morris RE: **Mechanochemically assisted hydrolysis in the ADOR process**. *Chem Sci* 2020, **11**:7060–7069, https://doi.org/10.1039/d0sc02547j.
The first demonstration of mechanochemical synthesis in the ADOR process.

21. Kasneryk V, Shamzhy M, Zhou J, Yue Q, Mazur M, Mayoral A, Luo Z, Morris RE, Čejka J, Opanasenko M: **Vapour-phase-transport rearrangement technique for the synthesis of new zeolites**. *Nat Commun* 2019, **10**:5129, https://doi.org/10.1038/s41467-019-12882-3.

22. * * Henkelis SE, Mazur M, Rice CM, Wheatley PS, Ashbrook SE, Morris RE: **Kinetics and mechanism of the hydrolysis and rearrangement processes within the assembly-disassembly-organization-reassembly synthesis of zeolites**. *J Am Chem Soc* 2019, **141**:4453–4459, https://doi.org/10.1021/jacs.9b00643.

A major study of the mechanism of the ADOR process showing how the short- and long-range structures of the materials develop throughout the reaction.

23. Morris SA, Wheatley PS, Položij M, Nachtigall P, Eliasova P, Cejka J, Lucas TC, Hriljac JA, Pinar AB, Morris RE: **Combined PDF and Rietveld studies of ADORable zeolites and the disordered intermediate IPC-1P**. *Dalton Trans* 2016, **45**: 14124–14130, https://doi.org/10.1039/C6DT02612E.

24. Jagiello J, Sterling M, Eliasova P, Opanasenko M, Zukal A, Morris RE, Navaro M, Mayoral A, Crivelli P, Warringham R, Mitchell S, Pérez-Ramírez J, Čejka J: **Structural analysis of IPC zeolites and related materials using positron annihilation spectroscopy and high-resolution argon adsorption**. *Phys Chem Chem Phys* 2016, **18**:15269–15277, https://doi.org/10.1039/C6CP01950A.

25. Trachta M, Bludsky O, Cejka J, Morris RE, Nachtigall P: **From double-four-ring germanosilicates to new zeolites: in silico investigation**. *ChemPhysChem* 2014, **15**:2972–2976, https://doi.org/10.1002/cphc.201402358.

26. Apperley DC, Harris RK, Hodgkinson P: *Solid-state NMR basic principles and practice*. New York: Momentum Press; 2012, https://doi.org/10.5643/9781606503522.

27. Duer MJ: *Solid-state NMR spectroscopy principles and applications*. Wiley; 2001, https://doi.org/10.1002/9780470999394.

28. Reif B, Ashbrook SE, Emsley L, Hong M: **Solid-state NMR spectroscopy**. *Nat. Rev. Methods Prim.* 2021, **1**:2, https://doi.org/10.1038/s43586-020-00002-1.

29. Lucier BEG, Chen S, Huang Y: **Characterization of metal-organic frameworks: unlocking the potential of solid-state NMR**. *Acc Chem Res* 2018, **51**:319–330, https://doi.org/10.1021/acs.accounts.7b00357.

30. Brunner E, Rauche M: **Solid-state NMR spectroscopy: an advancing tool to analyse the structure and properties of metal-organic frameworks**. *Chem Sci* 2020, **11**:4297–4304. https://doi.org/10/1039/D0SC00735H.

31. Li S, Lafon O, Wang W, Wang Q, Wang X, Li Y, Xu J, Deng F: **Recent advances of solid-state NMR spectroscopy for microporous materials**. *Adv Mater* 2020, 2002879, https://doi.org/10.1002/adma.202002879.

32. Zhao XL, Xu J, Deng F: **Solid-state NMR for metal-containing zeolites: from active sites to reaction mechanism**. *Front Chem Sci Eng* 2020, **14**:159–187, https://doi.org/10.1007/s11705-019-1885-1.

33. ** Ashbrook SE, Davis ZH, Morris RE, Rice CM: **^{17}O NMR spectroscopy of crystalline microporous materials**. *Chem Sci* 2021, **12**:5016–5036, https://doi.org/10.1039/D1SC00552A.
A summary of how ^{17}O NMR spectroscopy can be used to develop knowledge in porous materials of different kinds.

34. Frydman L, Harwood JS: **Isotropic spectra of half-integer quadrupolar spins from bidimensional magic-angle spinning NMR**. *J Am Chem Soc* 1995, **117**:5367–5368, https://doi.org/10.1021/ja00124a023.

35. Goldburt A, Madhu PK: **Multiple-quantum magic-angle spinning: high-resolution solid-state NMR of half-integer spin quadrupolar nuclei**. *Annu Rep NMR Spectrosc* 2005, **54**: 81–153, https://doi.org/10.1016/S0066-4103(04)54003-6.

36. Gan Z: **Isotropic NMR spectra of half-integer quadrupolar nuclei using satellite transitions and magic-angle spinning**. *J Am Chem Soc* 2000, **122**:3242–3243, https://doi.org/10.1021/ja9939791.

37. Ashbrook SE, Wimperis S: **High-resolution NMR of quadrupolar nuclei in solids: the satellite-transition magic angle spinning (STMAS) experiment**. *Prog Nucl Magn Reson Spectrosc* 2004, **45**:53–108, https://doi.org/10.1016/j.pnmrs.2004.04.002.

38. Pines A, Waugh JS, Gibby MG: **High-resolution NMR of quadrupolar nuclei in solids: the satellite-transition magic angle spinning (STMAS) experiment**. *J Chem Phys* 1972, **56**:1776, https://doi.org/10.1063/1.1677439.

39. Hartmann SR, Hahn EL: **Nuclear double resonance in the rotating frame**. *Phys Rev* 1962, **128**:2042–2053, https://doi.org/10.1103/PhysRev.128.2042.

40. Pickard CJ, Mauri F: **All-electron magnetic response with pseudopotentials: NMR chemical shifts**. *Phys Rev B Condens Matter* 2001, **63**, 245101, https://doi.org/10.1103/PhysRevB.63.245101.

41. Clark SJ, Segall MD, Pickard CJ, Hasnip PJ, Probert MIJ, Refson K, Payne MC: **First principles methods using CASTEP**. *Z Kristallogr* 2005, **220**:567–570, https://doi.org/10.1524/zkri.220.5.567.65075.

42. Bonhomme C, Gervais C, Babonneau F, Coelho C, Pourpoint F, Azais T, Ashbrook SE, Griffin JM, Yates JR, Mauri F, Pickard CJ: **First-principles calculation of NMR parameters using the gauge including projector augmented wave method: a chemist's point of view**. *Chem Rev* 2012, **112**:5733–5779, https://doi.org/10.1021/cr300108a.

43. Ashbrook SE, McKay DM: **Combining solid-state NMR spectroscopy with first-principles calculations – a guide to NMR crystallography**. *Chem Commun* 2016, **52**:7186–7204, https://doi.org/10.1039/c6cc02542k.

44. Charpentier T: **The PAW/GIPAW approach for computing NMR parameters: a new dimension added to NMR study of solids**. *Solid State Nucl Magn Reson* 2011, **40**:1–20. https://doi.org/10/106/j.ssnmr2011.04.006.

45. Martineau-Corcos C: **NMR Crystallography: a tool for the characterization of microporous hybrid solids**. *Curr Opin Colloid Interface Sci* 2018, **33**:35–43, https://doi.org/10.1016/j.cocis.2018.01.009.

46. MacKenzie KJD, Smith ME: *Multinuclear solid-state NMR of inorganic materials*. Pergamon, Oxford; 2002.

47. Paillaud J, Harbuzaru B, Patarin J, Bats N: **Extra-large-pore zeolites with two-dimensional channels formed by 14 and 12 rings**. *Science* 2004, **304**:990–993, https://doi.org/10.1126/science.1098242.

48. Corma A, Díaz-Cabañas MJ, Rey F, Nicolopoulus S, Boulahya K: **ITQ-15: the first ultralarge pore zeolite with a bi-directional pore system formed by intersecting 14- and 12-ring channels, and its catalytic implications**. *Chem Commun* 2004: 1356–1357, https://doi.org/10.1039/B406572G.

49. Shamzhy MV, Shvets OV, Opanasenko MV, Yaremov PS, Sarkisyan LG, Chlubná P, Zukal A, Marthala VR, Hartmann M, Čejka J: **Synthesis of isomorphously substituted extra-large pore UTL zeolites**. *J Mater Chem* 2012, **22**:15793–15803, https://doi.org/10.1039/C2JM31725G.

50. Přech J, Pizarro P, Serrano DP, Čejka J: **From 3D to 2D zeolite catalytic materials**. *Chem Soc Rev* 2018, **47**:8263–8306, https://doi.org/10.1039/C8CS00370J.

51. Roth WJ, Nachtigall P, Morris RE, Čejka J: **Two-dimensional zeolites: Current status and perspectives**. *Chem Rev* 2014, **114**:4807–4837, https://doi.org/10.1021/cr400600f.

52. Verheyen E, Joos L, Van Havenbergh K, Breynaert E, Kasian N, Gobechiya E, Houthoofd K, Martineau C, Hinterstein M, Taulelle F, Van Speybroeck V, Waroquier M, Bals S, Van Tendeloo G, Kirschhock CEA, Martens JA: **Design of zeolite by inverse sigma transformation**. *Nat Mater* 2012, **11**:1059–1064, https://doi.org/10.1038/nmat3455.

53. Li Q, Navrotsky A, Rey F, Corma A: **Thermochemistry of $(Ge_xSi_{1-x})O_2$ zeolites**. *Microporous Mesoporous Mater* 2003, **59**: 177–183, https://doi.org/10.1016/S1387-1811(03)00309-3.

54. Li Q, Navrotsky A, Rey F, Corma A: **Enthalpies of formation of Ge-zeolites: ITQ-21 and ITQ-22**. *Microporous Mesoporous Mater* 2004, **74**:87–92, https://doi.org/10.1016/j.micromeso.2004.06.010.

55. ** Kasian N, Tuel A, Verheyen E, Kirschhock CEA, Taulelle F, Martens JA: **NMR evidence for specific germanium siting in IM-12 zeolite**. *Chem Mater* 2014, **26**:5556–5565, https://doi.org/10.1021/cm502525w.
The authors showed how NMR can be used provide information on where germanium sits in zeolites. This is vitally important for understanding how the ADOR process works.

56. Jiang J, Yu J, Corma A: **Extra-large-pore zeolites: bridging the gap between micro and mesoporous structures**. *Angew Chem*

Int Ed 2010, **49**:3120–3145, https://doi.org/10.1002/anie.200904016.

57. Jiang J, Jorda JL, Diaz-Cabanas MJ, Yu J, Corma A: **The synthesis of an extra-large-pore zeolite with double three-ring building units and a low framework density**. *Angew Chem Int Ed* 2010, **49**:4986–4988, https://doi.org/10.1002/anie.20100506.

58. Roth WJ, Shvets OV, Shamzhy M, Chlubná P, Kubů M, Nachtigall P, Čejka J: **Postsynthesis transformation of three-dimensional framework into a lamellar zeolite with modifiable architecture**. *J Am Chem Soc* 2011, **133**:6130–6133, https://doi.org/10.1021/ja200741r.

59. Henkelis SE, Morris SA, Mazur M, Wheatley PS, McHugh LN, Morris RE: **Monitoring the assembly–disassembly–organisation–reassembly process of germanosilicate UTL through *in situ* pair distribution function analysis**. *J Mater Chem* 2018, **6**:17011–17018, https://doi.org/10.1039/C8TA04320E.

60. Russell SE, Henkelis SE, Vornholt SM, Rainer DN, Chapman KW, Morris RE: ***In situ* flow pair distribution function analysis to probe the assembly–disassembly–organisation–reassembly (ADOR) mechanism of zeolite IPC-2 synthesis**. *Mater. Adv.* 2021, **2**:7949–7955, https://doi.org/10.1039/D1MA00335F.

61. Xu H, Jiang J, Yang B, Zhang L, He M, Wu P: **Post-synthesis treatment gives highly stable siliceous zeolites through the isomorphous substitution of silicon for germanium in germanosilicates**. *Angew Chem Int Ed* 2014, **53**:1355–1359, https://doi.org/10.1002/anie.201306527.

62. ** Bignami GPM, Dawson DM, Seymour VR, Wheatley PS, Morris RE, Ashbrook SE: **Synthesis, isotopic enrichment, and solid-state NMR characterization of zeolites derived from the assembly, disassembly, organization, reassembly process**. *J Am Chem Soc* 2017, **139**:5140–5148, https://doi.org/10.1021/jacs.7b00386.
The authors showed how ^{17}O enrichment could be accomplished during ADOR and how this can be used to give new information on the overall mechanism of the process.

63. ** Morris SA, Bignami GPM, Tian Y, Navarro M, Firth DS, Čejka J, Wheatley PS, Dawson DM, Slawinski WA, Wragg DS, Morris RE, Ashbrook SE: **In situ solid-state NMR and XRD studies of the ADOR process and the unusual structure of zeolite IPC-6**. *Nat Chem* 2017, **9**:1012–1018, https://doi.org/10.1038/nchem.2761.
The first *in situ* NMR study of the ADOR process.

64. Mazur M, Arévalo-López AM, Wheatley PS, Bignami GPM, Ashbrook SE, Morales-García Á, Nachtigall P, Attfield JP, Čejka J, Morris RE: **Pressure-induced chemistry for the 2D to 3D transformation of zeolites**. *J Mater Chem* 2018, **6**:5255–5259, https://doi.org/10.1039/c7ta09248b.

65. Ma Y, Xu H, Liu X, Peng M, Mao W, Han L, Jiang J, Wu P: **Structural reconstruction of germanosilicate frameworks by controlled hydrogen reduction**. *Chem Commun* 2019, **55**:1883–1886, https://doi.org/10.1039/c8cc09294j.

66. Kasneryk V, Opanasenko M, Shamzhy M, Musilová Z, Avadhut YS, Hartmann M, Čejka J: **Consecutive interlayer disassembly–reassembly during alumination of UOV zeolites: insight into the mechanism**. *J Mater Chem* 2017, **5**:22576–22587, https://doi.org/10.1039/C7TA05935C.

67. Liu X, Ravon U, Tuel A: **Fluoride removal from double four-membered ring (D4R) units in as-synthesized Ge-containing zeolites**. *Chem Mater* 2011, **23**:5052–5057, https://doi.org/10.1021/cm2025735.

68. Liu X, Ravon U, Tuel A: **Evidence for F^-/SiO^- anion exchange in the framework of as-synthesized all-silica zeolites**. *Angew Chem Int Ed* 2011, **50**:5900–5903, https://doi.org/10.1002/anie.201101237.

69. Liu X, Ravon U, Bosselet F, Bergeret G, Tuel A: **Probing Ge distribution in zeolite frameworks by post-synthesis introduction of fluoride in as-made materials**. *Chem Mater* 2012, **24**:3016–3022, https://doi.org/10.1021/cm301511y.

70. Shamzhy M, Opanasenko M, Tian Y, Konysheva K, Shvets O, Morris RE, Čejka J: **Germanosilicate precursors of ADORable zeolites obtained by disassembly of ITH, ITR, and IWR zeolites**. *Chem Mater* 2014, **26**:5789–5798, https://doi.org/10.1021/cm502953s.

71. Shvets OV, Shamzhy MV, Yaremov PS, Musilová Z, Procházková D, Čejka J: **Isomorphous introduction of boron in germanosilicate zeolites with UTL topology**. *Chem Mater* 2011, **23**, 25732585, https://doi.org/10.1021/cm200105f.

72. Shvets OV, Nachtigall P, Roth WJ, Cejka J: **UTL zeolite and the way beyond**. *Microporous Mesoporous Mater* 2013, **182**:229–238, https://doi.org/10.1016/j.micromeso.2013.03.023.

73. Shamzhy MV, Eliašová P, Vitvarová D, Opanasenko MV, Firth DS, Morris RE: **Post-synthesis stabilization of germanosilicate zeolites ITH, IWW, and UTL by substitution of Ge for Al**. *Chem Eur J* 2016, **22**:17377–17386, https://doi.org/10.1002/chem.201603434.

74. Zhang J, Veselý O, Tošner Z, Mazur M, Opanasenko M, Čejka J, Shamzhy M: **Toward controlling disassembly step within the ADOR process for the synthesis of zeolites**. *Chem Mater* 2021, **33**:1228–1237, https://doi.org/10.1021/acs.chemmater.0c03993.

75. Métro T-X, Gervais C, Martinez A, Bonhomme C, Laurencin D: **Unleashing the potential of ^{17}O NMR spectroscopy using mechanochemistry**. *Angew Chem Int Ed* 2017, **56**:6803–6807, https://doi.org/10.1002/anie.201702251.

76. ** Chen CH, Gaillard E, Mentink-Vigier F, Chen K, Gan Z, Gaveau P, Rebiere B, Berthelot R, Florian P, Bonhomme C, Smith ME, Métro T-X, Alonso B, Laurencin D: **Direct ^{17}O isotopic labeling of oxides using mechanochemistry**. *Inorg Chem* 2020, **59**:13050–13066, https://doi.org/10.1021/acs.inorgchem.0c00208.
The authors combine ^{17}O NMR spectroscopy and mechanochemistry to provide direct study of enriched oxides.

77. Chen CH, Mentink-Vigier F, Trebosc J, Goldberga I, Gaveau P, Thomassot E, Iuga D, Smith ME, Chen K, Gan Z, Fabregue N, Métro T-X, Alonso B, Laurencin D: **Labeling and probing the silica surface using mechanochemistry and ^{17}O NMR spectroscopy**. *Chem Eur J* 2021, **49**:12574–12588, https://doi.org/10.1002/chem.202101421.

78. Hussin R, Dupree R, Holland D: **The Ge-O-Ge bond angle distribution in GeO_2 glass: a NMR determination**. *J Non-Cryst Solids* 1999, **246**:159–168, https://doi.org/10.1016/S0022-3093(99)00090-3.

79. Zhang J, Yue Q, Mazur M, Opanasenko M, Shamzhy MV, Čejka J: **Selective recovery and recycling of germanium for the design of sustainable zeolite catalysts**. *ACS. Chem. Eng.* 2020, **8**:8235–8246, https://doi.org/10.1021/acssuschemeng.0c01336.

80. ** Pugh SM, Wright PA, Law DJ, Thompson N, Ashbrook SE: **Facile, room-temperature ^{17}O enrichment of zeolite frameworks revealed by solid-state NMR spectroscopy**. *J Am Chem Soc* 2020, **142**:900–906, https://doi.org/10.1021/jacs.9b10528.
^{17}O NMR spectroscopy used to demonstrate how oxygen exchange in a zeolite is relatively easy when in the presence of water.

81. Rossini AJ, Zagdoun A, Lelli M, Lesage A, Coperet C, Emsley L: **Dynamic nuclear polarization surface enhanced NMR spectroscopy**. *Acc Chem Res* 2013, **46**:1942–1951, https://doi.org/10.1021/ar300322x.

82. Thankamony ASL, Wittmann JJ, Kaushik M, Corzilius B: **Dynamic nuclear polarization for sensitivity enhancement in modern solid-state NMR**. *Prog Nucl Magn Reson Spectrosc* 2017, **102–103**:120–195, https://doi.org/10.1016/j.pnmrs.2017.06.0022.

83. Chow WY, DePaepe G, Hediger S: **Biomolecular and biological applications of solid-state NMR with dynamic nuclear polarization enhancement**. *Chem Rev* 2022, **122**:9795–9847, https://doi.org/10.1021/acs.chemrev.1c01043.

84. Moroz IB, Leskes M: **Dynamic nuclear polarization solid-state NMR spectroscopy for materials research**. *Annu Rev Mater Res* 2022, **52**:25–55, https://doi.org/10.1146/annurev-matsci-081720-085634.

85. Ashbrook SE, Morris RE, Rice CM: *Understanding the synthesis and reactivity of ADORable zeolites using NMR spectroscopy (datset)*. Dataset. University of St Andrews Research Portal; 2022, https://doi.org/10.17630/d82e58e4-b4a0-40b3-8156-5cbf80eeea72.